Geophysical Research Letters

RESEARCH LETTER
10.1029/2023GL103342

MLT Dependence of Relativistic Electron Scattering Into the Drift Loss Cone: Measurements From ELFIN-L on Board Lomonosov Spacecraft

Yuri Y. Shprits[1,2,3], Ingo Michaelis[1], Dedong Wang[1], Hayley Allison[1], Ruggero Vasile[1,4], Andrei Runov[2], Alexander Drozdov[2], Christopher T. Russell[2], Vladimir Kalegaev[5], and Artem Smirnov[1,3]

[1]GFZ German Research Centre for Geosciences, Potsdam, Germany, [2]University of California Los Angeles, Los Angeles, CA, USA, [3]Institute for Physics and Astronomy, University of Potsdam, Potsdam, Germany, [4]Now at Meta Platforms, Inc, Menlo Park, CA, USA, [5]Moscow State University, Moscow, Russia

Abstract There have been a number of theories proposed concerning the loss of relativistic electrons from the radiation belts. However, direct observations of loss were not possible on a number of previous missions due to the large field of view of the instruments and often high-altitude orbits of satellites that did not allow researchers to isolate the precipitating electrons from the stably trapped. We use measurements from the ELFIN-L suit of instruments flown on Lomonosov spacecraft at LEO orbit, which allows us to distinguish stably trapped from the drift loss cone electrons. The sun-synchronous orbit of Lomonosov allows us to quantify scattering that occurred into the loss cone on the dawn-side and the dusk-side magnetosphere. The loss at MeV energies is observed predominantly on the dawn-side, consistent with the loss induced by the chorus waves. The companion data publication provides processed measurements.

Plain Language Summary There have been a number of models proposed concerning the loss of relativistic electrons from radiation belts. However, the direct observations of loss have been missing, as for most of the previous missions; the large aperture telescopes could not isolate the precipitating electrons from being stably trapped. In this study, we use measurements from ELFIN-L on Lomonosov that allow for such separation and allow us to distinguish stably trapped from precipitating particles. We can also identify the particles that will be lost within one drift around the Earth, the so-called drift loss cone. For understanding the loss processes and differentiating between them, it's crucially important to quantify where in local magnetic time these electrons will be scattered into the drift loss cone. Measurements from the ELFIN-L instrument show that the loss at MeV energies is observed predominantly on the dawn side, consistent with the loss induced by the so-called chorus plasma waves.

Key Points:

- ELFIN-L measurements allow comparing scattering into the loss cone on the dawn and dusk side
- Processed Level-3 measurements are provided in the data publication
- Most of the relativistic electrons are scattered into the drift loss cone on the dawn side

Supporting Information:

Supporting Information may be found in the online version of this article.

Correspondence to:

Y. Y. Shprits,
yshprits@gfz-potsdam.de

Citation:

Shprits, Y. Y., Michaelis, I., Wang, D., Allison, H., Vasile, R., Runov, A., et al. (2023). MLT dependence of relativistic electron scattering into the drift loss cone: Measurements from ELFIN-L on board Lomonosov spacecraft. *Geophysical Research Letters*, *50*, e2023GL103342. https://doi.org/10.1029/2023GL103342

Received 13 MAR 2023
Accepted 5 JUN 2023

Author Contributions:

Conceptualization: Yuri Y. Shprits
Data curation: Yuri Y. Shprits, Ingo Michaelis
Formal analysis: Yuri Y. Shprits, Ingo Michaelis
Funding acquisition: Yuri Y. Shprits
Investigation: Yuri Y. Shprits, Ingo Michaelis
Methodology: Yuri Y. Shprits
Project Administration: Yuri Y. Shprits
Resources: Yuri Y. Shprits
Software: Yuri Y. Shprits, Ingo Michaelis, Ruggero Vasile
Supervision: Yuri Y. Shprits
Validation: Yuri Y. Shprits, Ingo Michaelis, Dedong Wang, Hayley Allison, Ruggero Vasile, Artem Smirnov

1. Introduction

Significant advances in the understanding of the acceleration of the radiation belt particles have been obtained due to historical measurements on CRRES satellite (Johnson & Kierein, 1992) and new measurements provided by the Van Allen Probes mission (Mauk et al., 2012). The mechanisms for the acceleration of relativistic electrons were validated by the newly developed codes solving the full three-dimensional Fokker-Planck equation, such as ONERA Salammbô code (Varotsou et al., 2008), the British Antarctic Survey (BAS) Radiation Belt Code (e.g., Allison et al., 2019; Glauert et al., 2014a, 2014b; Kersten et al., 2014), the Versatile Electron Radiation Belt (VERB) code (e.g., Drozdov et al., 2017; Kim et al., 2012; Shprits, Subbotin, et al., 2008; Shprits et al., 2009; Subbotin et al., 2010, 2011; Subbotin & Shprits, 2009; Wang et al., 2020; Wang & Shprits, 2019) and DREAM-3D code (e.g., Reeves et al., 2012; Tu et al., 2013). Various combinations of 1-D, 2D or combination of convection and 2D simulations have also been presented in recent studies (e.g., Fok et al., 2011; Li et al., 2016; Ripoll et al., 2019). Advances in modeling and observations have allowed us to significantly advance our understanding of the acceleration mechanisms in the radiation belts (Millan & Thorne, 2007; Shprits, Subbotin, et al., 2008; Shprits, Elkington, et al., 2008; Shprits et al., 2022; Thorne, 2010). The proposed dominant scattering mechanisms are: scattering by VLF/ELF hiss waves that occur inside the plasmasphere at practically all MLT (Lyons & Thorne, 1973) and in the regions of plumes (e.g., Li et al., 2007), whistler-mode chorus waves (Li et al., 2007; Miyoshi et al., 2020, 2021; Shprits, Subbotin, et al., 2008; Shumko et al., 2021; Thorne et al., 2005;

Visualization: Yuri Y. Shprits, Ingo Michaelis, Artem Smirnov
Writing – original draft: Yuri Y. Shprits
Writing – review & editing: Yuri Y. Shprits, Ingo Michaelis, Dedong Wang, Hayley Allison, Ruggero Vasile, Andrei Runov, Alexander Drozdov, Christopher T. Russell, Vladimir Kalegaev, Artem Smirnov

Tsai et al., 2022; Wang & Shprits, 2019; Zhang et al., 2022), EMIC waves predominantly on the dusk side in the regions of plumes or on the edge of the plasmasphere (Thorne & Kennel., 1971) and the loss to the magnetopause that drives the outward radial diffusion (Shprits et al., 2006; Staples et al., 2022; Turner et al., 2012; Wang et al., 2020). However, the understanding of loss processes is still incomplete. Fundamental questions about the loss of electrons remain to be debated and the direct observational evidence for several proposed loss mechanisms (Shprits, Subbotin, et al., 2008; Shprits, Elkington, et al., 2008) remains lacking. In particular, it remains unclear what loss process dominates the scattering into the atmosphere at MeV energies.

To directly evaluate the loss of electrons from the radiation belts, measurements should be able to accurately resolve the loss cone and distinguish between the quasi-trapped, trapped, and precipitating populations, which is difficult to achieve from a near-equatorial orbit where recent satellite missions operated. In particular, one of the most compelling questions related to loss is where does the scattering of the radiation belt elections occur? Answering these questions can help identify the wave modes and physical mechanisms responsible for such scattering.

In this study, we utilize the measurements from the electron particle detector (EPD) of the ELFIN-L instrument suite (Shprits et al., 2018) that has been flown on the Lomonosov spacecraft. The satellite was launched on 28 April 2016 into a polar, sun-synchronous orbit. The inclination was 97.3° at a mean altitude of about 485 km. The orbit period is 94.2 min. The orbit of the Lomonosov satellite allows us to routinely sample and compare the measurements in the vicinity of noon and midnight (11.11 ± 1.64 and 23.27 ± 1.68). EPD was designed to have a relatively narrow field of view (22.5°), to be able to differentiate between Drift Loss Cone (DLC), Bounce Loss Cone (BLC), and Trapped populations. The data rate is two measurements per second on eight physical electron detectors with 12 sub-channels from 21 keV to 4.7 MeV. The data is available from August to November 2016. Some of the electron detector channels do not show valid measurements, most likely due to insufficient particle counts (Shprits et al., 2018). The useable channels are with central energies of 21 keV, 30 keV, 44 keV, 1.006 MeV, and 1.600 MeV.

2. Data Processing

To understand the loss of electrons, we, first of all, need to understand if the instruments are measuring stably trapped fluxes, locally precipitating fluxes or particles that will be lost within one drift orbit in the region where the magnetic field will be weak enough so that the mirror point will be lowered to the level of the atmosphere. Such particles that are lost during one drift orbit are referred to as particles in the drift loss cone (DLC), and particles that will precipitate locally on the time scale of one bounce are referred to as particles in the bounce loss cone (BLC). To identify the BLC, the magnetic field where particle mirrors B_m should be calculated from the instrument look direction and the spacecraft local magnetic field which is estimated by using the IGRF model. The mirror point magnetic field should be compared to an estimated magnetic field at the top of the atmosphere or footprint of the field line $B_{\text{foot,}}$ which for this study, we assume to be at 100 km. If B_m is lower than B_{foot} the particle will mirror above the atmosphere where the magnetic field is lower than in the atmosphere and will not be lost during the bounce. If B_m is higher than B_{foot}, the particle will be lost during the bounce motion and should be labeled as BLC.

To identify the DLC measurements the magnetic field at the mirror point (e.g., Roederer & Zhang, 2014), which is conserved along the drift path due to the conservation of the second adiabatic invariant, should be compared with the minimum magnetic field that the particle will encounter along the entire drift motion. If the mirror point magnetic field B_m is greater than the minimum value of the magnetic field at 100 km for a given L-shell $B_{\text{drift\_min}}$, then the particle will be lost over the drift orbit and should be labeled as DLC. If B_m is smaller than $B_{\text{drift\_min}}$ the particle will be stably trapped and in the absence of pitch angle diffusion, will not be lost from the system.

We have pre-calculated B_{foot} as a function of McIlwain Lm (McIlwain, 1961) and quasi-dipole longitude (QDLON) using International Geomagnetic Reference Field (IGRF) 12 (Thébault et al., 2015) geomagnetic model. The field lines are traced using International Radiation Belt Environment Modeling (IRBEM) library version 6.1.2 (Boscher et al., 2013). The minimum between the northern and southern hemispheres of B_{foot}, is shown on Figure 1.

The method was validated by reproducing the previously published results in (Tu et al., 2009), see Figure S1 in Supporting Information S1. The Geodetic coordinates (GDZ) are calculated from the Geographic Coordinate

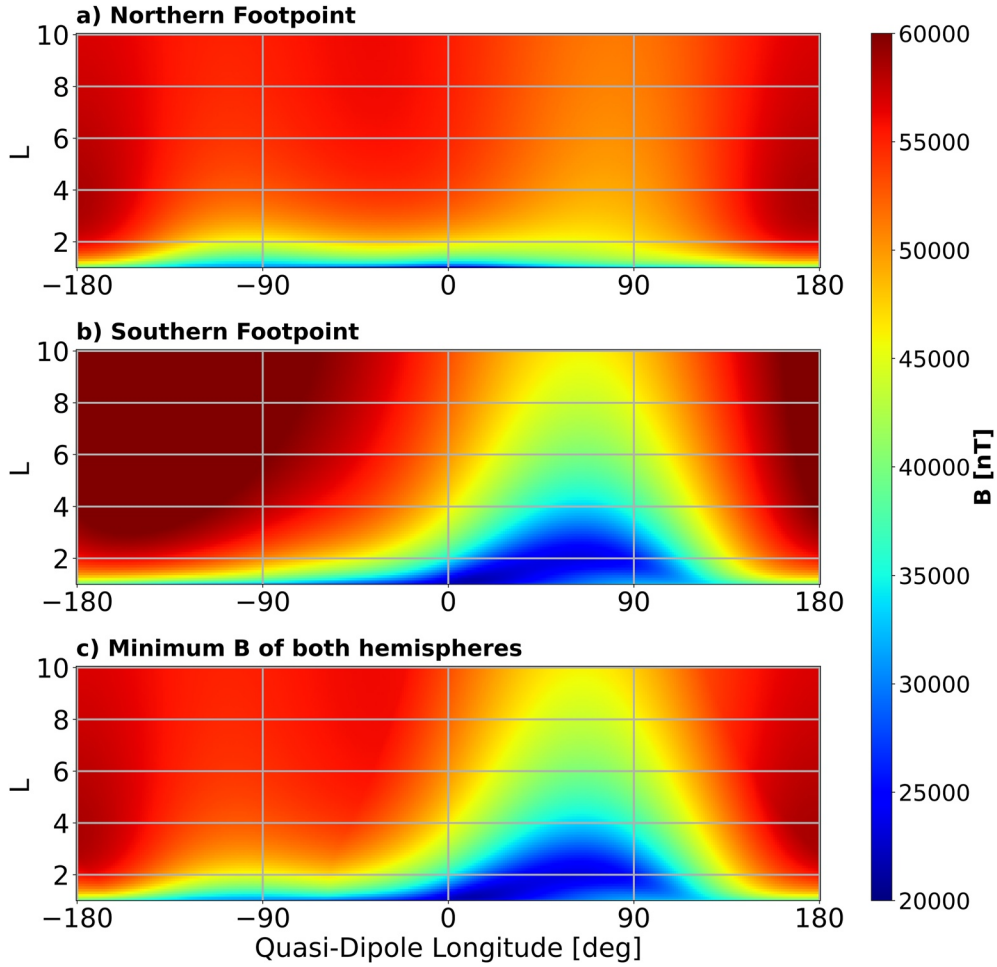

Figure 1. Calculated (a) northern magnetic footpoint, (b) southern magnetic footpoint and (c) smallest of the northern and southern hemisphere magnetic foot point, at the altitude of 100 km as a function of L and quasi-dipole longitude (IGRF).

system (GEO) using the IRBEM library. Position in these coordinates is used to calculate the QDLON using the "apexpy" which is a Python wrapper for the Apex Fortran library based on Richmond (1995) and Emmert et al. (2010). For the calculation of Lm we use McIlwain's look-up table (McIlwain, 1961), which calculates Lm from invariant I and B_m values. B_m can be calculated using the IRBEM library. For the calculation of invariant and tracing field lines, we use an approach by Orlova and Shprits (2011). Using the pre-calculated B_{foot} and McIlwain Lm and QDLON at each satellite position and pre-calculated table as discussed above, we determine if we measure particles in the DLC.

To compare dawn and dusk-side scattering, we need to compare measurements on the day and night sides at the same geographic location. The DLC measurements on the day and night side can only be observed in the Alaska geographic sector, and for this study, we focus on measurements over this geographic location. Another complication comes from the fact that the instrument has a finite field of view, and each corner of the instrument's aperture is associated with a slightly different pitch angle. The estimates that are usually done for the central angle of the instrument field of view may be deceptive as even a small amount of trapped particles may by far outnumber the measured drift loss cone or bounce loss cone particles and can significantly contaminate the measurements. As the focus of this study is the drift loss cone population, we chose the most conservative estimates and checked that all four corners of the instrument satisfy the DLC condition when determining the measurements that we assigned to DLC. The same conservative approach is applied to the determination of the BLC. We consider a measurement to be in the BLC only when all four vectors go through the corners of the instrument point into the BLC.

The L3 data set (Shprits & Michaelis, 2023) contains additional information of B_m, B_{foot}, B_{eq} as well as flags for BLC and DLC.

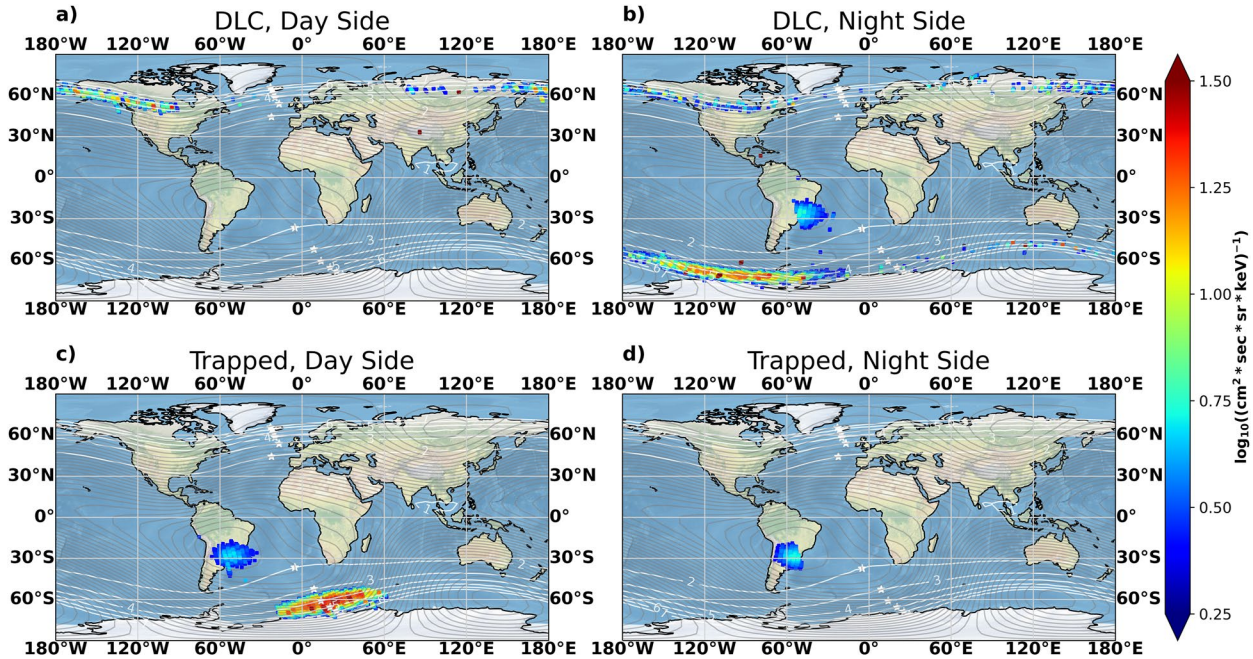

Figure 2. Scatter plot for ELFIN-L measured differential electron flux at 1,006 keV from August to November 2016. The top row shows drift loss cone measurements for (a) day-side, (b) night-side, and the bottom row trapped electrons measured on the day side (c) and night side (d). Gray lines show contours of magnetic field intensity, while white lines show contours of Lm. White stars show the location of $B_{\text{foot\_min}}$ along iso-lines of Lm. For DLC on the day side, (a) we focused on the northern hemisphere since a clean distinction between DLC and trapped is difficult for the southern hemisphere.

3. Results

3.1. Separating Different Populations Near the Edge of the Loss Cone

Using the methodology as discussed above, we have separated all the measurements into BLC, DLC, and trapped. Figure 2 shows the DLC and trapped populations. As the ELFIN-L direction is inclined at 60° with respect to the plane defined by zenith and satellite velocity, the orientation of the instrument allows us to measure various populations of particles at different geographical locations. In the outer belt, trapped fluxes were only observed in the southern hemisphere near the minimum in the magnetic field along the lines of constant L-shell. Trapped fluxes are also observed in the inner belt and may be contaminated by the highly energetic trapped protons. The trapped outer belt fluxes are most clearly seen around longitudes of Africa on the day side. The DLC fluxes can be observed in the northern and southern hemispheres. Clearly seen is the trend of increasing fluxes as electrons drift eastwards, and more particles can be scattered into the DLC before they are lost in the region close to the minimum magnetic field, which is marked by stars on the constant Lm contour white lines.

3.2. Comparison of the Dawn and Dusk-Side Scattering

The orbit of Lomonosov allows for comparing measurements on the night side with the measurements on the day side. The measurements of DLC fluxes on the night side will be dominated by particles that were scattered into the loss cone on the dawn side, and the measurements on the day side will be dominated by the particles that were scattered on the dusk side as electrons are drifting eastward. The exact range of MLT at which electrons may be scattered into the DLC will depend on the MLT of the minimum B for a given Lm. In particular, all electrons may be scattered in the loss cone westward of the point where the measurement is made and westward of the minimum B. The minimum B for a given L-shell we henceforth refer to as South Atlantic Anomaly (SAA) as the latitude of the SAA approximately coincides with the minimum B for a given Lm (see stars depicting minimum B in Figure 2).

To further confine the region where particles can be scattered into the loss cone, we choose SAA to be on the dusk side when we are considering the measurements on the day side so that we can observe the scattering into the DLC that occurred on the dawn side. Similarly, when observing the night side DLC fluxes, we only consider

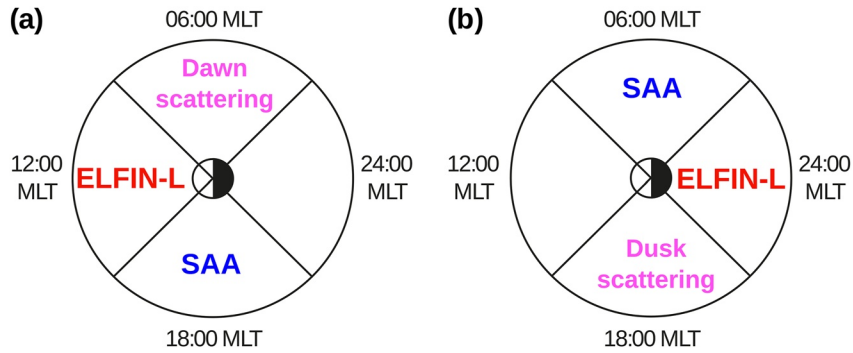

Figure 3. Definition of (a) Dawn and (b) Dusk precipitation with respect to local time location of ELFIN-L and South Atlantic Anomaly.

measurements when SAA is on the dawn side so that we can be sure that the scattering occurred westward of the SAA. Figure 3 shows how SAA location is restricted for the day-side and night-side measurements. Such selection of SAA does not entirely limit the scattering to the dawn or dusk side. Ideally, SAA should be located at noon for the near-midnight measurements and at midnight for the near-dayside measurements. However, such restriction would eliminate most of the measurements and would not allow obtaining statistically significant results. Such analysis should be possible in the future for longer-term missions such as ELFIN (Angelopoulos et al., 2020).

Figure 4c shows that the scattering over the dawn side exceeds the scattering over the dusk side. Such a scenario is consistent with loss of electrons mostly due to chorus waves. It is difficult to exactly quantify this ratio due to the lack of data; some measurements of the dawn side precipitation may be mixed with the dusk side precipitation and vice versa, as discussed above. Similar observations and similar conclusions have been made by Allison et al. (2017) but for lower energy electrons using Polar Operational Environmental Satellite (POES) measurements. Exactly the same analysis has been conducted for the NOAA POES-19 measurements and is presented in Figure S3 in Supporting Information S1. Additional statistics information about the measurements per bin for Figure 4 is shown in Figure S5 in Supporting Information S1 and briefly described in Text S5 in Supporting Information S1.

4. Summary and Discussion

In this study, we performed a statistical analysis of the data collected from the ELFIN-L instrument on board the Lomonosov spacecraft. The small field of view of the instrument provides a unique opportunity to clearly separate the BLC, DLC, and trapped electron fluxes. Separating the populations of BLC, DLC, and trapped is a

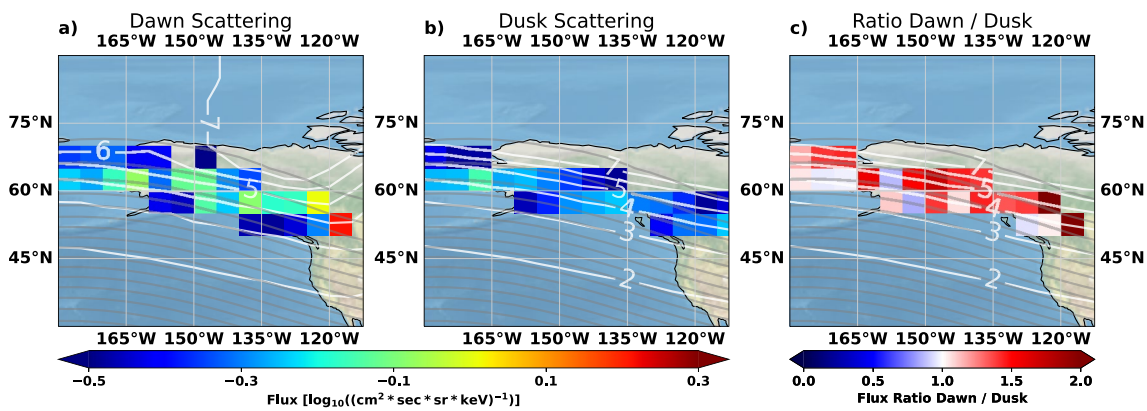

Figure 4. ELFIN-L differential Flux at 1,006 keV in log10((cm^2 × sec × sr × keV)$^{-1}$) from August to November 2016 over Alaska measuring electrons in the DLC that were predominantly scattered in the (a) dawn sector and (b) dusk sector. Panel (c) shows the ratio between Dawn and Dusk precipitation. White lines show contours of Lm; gray lines show contours of magnetic field intensity. The noise level has been cut at −0.5 log10((cm^2 × sec × sr × keV)$^{-1}$).

technically challenging task and requires careful consideration of the geometry of the instrument and exclusion of the geographic locations where all three populations can be simultaneously observed, and measurements are difficult to classify as either of these populations as most of them contain a mixture of populations. The observed trapped fluxes maximize around the minimum in the magnetic field consistent with the physical expectations. The observed statistical DLC fluxes increase as electrons drift eastwards, increasing up to the minimum B along the given L-shell before showing a sudden drop close to the minimum B point, also consistent with physical expectations. This seemingly obvious sanity check should be performed for similar analysis in future studies to verify that the inferred precipitating fluxes are, in fact, realistic and are not contaminated by the trapped fluxes that can exceed the precipitating fluxes by several orders of magnitude.

It should be noted that this study focuses on the scattering into the drift loss cone. Very fast scattering can occur due to non-linear scattering and bounce loss cone fluxes may even exceed the trapped fluxes (Zhang et al., 2022). Such superfast precipitation cannot be identified with the ELFIN-L instrument and requires a spinning spacecraft that can observe all pitch angles. A very localized and short-lived very fast scattering on the dusk side may be also potentially overlooked by this statistical study.

Our findings show that in a statistical sense, the dawn side scattering into the drift loss cone is much more efficient than the dusk side scattering. That is an indication that at the MeV energies, chorus waves that are observed predominantly on the dawn side provide more scattering into the drift loss cone than EMIC waves that are observed on the dusk side. These findings are also consistent with the conclusions of Shprits et al. (2013, 2016, 2017, 2022), Drozdov et al. (2015, 2017, 2020, 2022), Aseev et al. (2017), Qin et al. (2019), and Usanova et al. (2014) who argued that EMIC waves are most efficient at multi-MeV and not very efficient at MeV energies. Similar results are obtained using the POES satellite data and presented in Supporting Information S1.

The companion data publications provide all Level 1, 2, and 3 data, including flagged data points that would allow to reproduce of this investigation and conduct additional investigations of individual events and conjunction studies.

Data Availability Statement

All data used can be found in the accompanying data publications Michaelis and Shprits (2023a, 2023b, 2023c, 2023d, 2023e), and Shprits and Michaelis (2023). NOAA POES data that is used in Supporting Information S1 of this study is publicly available and can be obtained from https://www.ncei.noaa.gov/data/poes-metop-space-environment-monitor/access/l1b/v01r00/.

Acknowledgments
This project was supported by the National Science Foundation (NSF) RAPID GRANT: Adding Energetic Particle and Magnetic Field Measurements to a Russian University Satellite Mission AGS#1013218 and by the Helmholtz Association. We acknowledge the use of the IRBEM library (6.1.2), the latest version of which can be found at https://doi.org/10.5281/zenodo.6867552. This project has received funding from the European Union's Horizon 2020 research and innovation program under grant agreement No. 870452 (PAGER). We would like to acknowledge the contribution of Prof. Mikhail Panasyuk; and Prof. Angelopoulos without who's leadership and contributions, this study would not have been possible. Open Access funding enabled and organized by Projekt DEAL.

References

Allison, H. J., Horne, R. B., Glauert, S. A., & Del Zanna, G. (2019). On the importance of gradients in the low-energy electron phase space density for relativistic electron acceleration. *Journal of Geophysical Research: Space Physics*, *124*, 2628–2642. https://doi.org/10.1029/2019ja026516

Allison, H. J., Horne, R. B., Glauert, S. A., & Zanna, G. D. (2017). The magnetic local time distribution of energetic electrons in the radiation belt region. *Journal of Geophysical Research: Space Physics*, *122*(8), 8108–8123. https://doi.org/10.1002/2017JA024084

Angelopoulos, V., Tsai, E., Bingley, L., Shaffer, C., Turner, D. L., Runov, A., et al. (2020). The ELFIN mission. *Space Science Reviews*, *216*(5), 103. https://doi.org/10.1007/s11214-020-00721-7

Aseev, N., Shprits, Y., Drozdov, A. Y., Kellerman, A. C., Usanova, M. E., Wang, D., & Zhelavskaya, I. (2017). Signatures of ultrarelativistic electron loss in the heart of the outer radiation belt measured by Van Allen Probes. *Journal of Geophysical Research*, *122*(10), 10102–10111. https://doi.org/10.1002/2017JA024485

Boscher, D., Bourdarie, S., O'Brien, T. P., & Guild, T. (2013). The international radiation belt environment modeling (IRBEM) library. Retrieved from http://sourceforge.net/projects/irbem

Drozdov, A. Y., Allison, H. J., Shprits, Y., Usanova, M. E., Saikin, A., & Wang, D. (2022). Depletions of multi-MeV electrons and their association to minima in phase space density. *Geophysical Research Letters*, *49*(8), e2021GL097620. https://doi.org/10.1029/2021GL097620

Drozdov, A. Y., Shprits, Y. Y., Orlova, K. G., Kellerman, A. C., Subbotin, D. A., Baker, D. N., et al. (2015). Energetic, relativistic, and ultrarelativistic electrons: Comparison of long-term VERB code simulations with Van Allen Probes measurements. *Journal of Geophysical Research: Space Physics*, *120*(5), 3574–3587. https://doi.org/10.1002/2014JA020637

Drozdov, A. Y., Shprits, Y. Y., Usanova, M. E., Aseev, N. A., Kellerman, A. C., & Zhu, H. (2017). EMIC wave parameterization in the long-term VERB code simulation. *Journal of Geophysical Research: Space Physics*, *122*(8), 8488–8501. https://doi.org/10.1002/2017JA024389

Drozdov, A. Y., Usanova, M. E., Hudson, M. K., Allison, H. J., & Shprits, Y. Y. (2020). The role of hiss, chorus, and EMIC waves in the modeling of the dynamics of the multi-MeV radiation belt electrons. *Journal of Geophysical Research: Space Physics*, *125*(9), 2628. https://doi.org/10.1029/2020JA028282

Emmert, J. T., Richmond, A. D., & Drob, D. P. (2010). A computationally compact representation of Magnetic Apex and Quasi-Dipole coordinates with smooth base vectors. *Journal of Geophysical Research*, *115*(A8), A08322. https://doi.org/10.1029/2010JA015326

Fok, M.-C., Glocer, A., Zheng, Q., Horne, R. B., Meredith, N. P., Albert, J. M., & Nagai, T. (2011). Recent developments in the radiation belt environment model. *Journal of Atmospheric and Solar-Terrestrial Physics*, *73*(11), 1435–1443. https://doi.org/10.1016/j.jastp.2010.09.033

Glauert, S. A., Horne, R. B., & Meredith, N. P. (2014a). Simulating the Earth's radiation belts: Internal acceleration and continuous losses to the magnetopause. *Journal of Geophysical Research: Space Physics*, *119*(9), 7444–7463. https://doi.org/10.1002/2014ja020092

Glauert, S. A., Horne, R. B., & Meredith, N. P. (2014b). Three-dimensional electron radiation belt simulations using the BAS radiation belt model with new diffusion models for chorus, plasmaspheric hiss, and lightning-generated whistlers. *Journal of Geophysical Research: Space Physics*, *119*(1), 268–289. https://doi.org/10.1002/2013ja019281

Johnson, M., & Kierein, J. (1992). Combined release and radiation effects satellite (CRRES): Spacecraft and mission. *Journal of Spacecraft and Rockets*, *29*(4), 556–563. https://doi.org/10.2514/3.55641

Kersten, T., Horne, R. B., Glauert, S. A., Meredith, N. P., Fraser, B. J., & Grew, R. S. (2014). Electron losses from the radiation belts caused by EMIC waves. *Journal of Geophysical Research: Space Physics*, *119*(11), 8820–8837. https://doi.org/10.1002/2014JA020366

Kim, K.-C., Shprits, Y., Subbotin, D., & Ni, B. (2012). Relativistic radiation belt electron responses to GEM magnetic storms: Comparison of CRRES observations with 3-D VERB simulations. *Journal of Geophysical Research*, *117*(A8), A08221. https://doi.org/10.1029/2011JA017460

Li, W., Ma, Q., Thorne, R. M., Bortnik, J., Zhang, X.-J., Li, J., et al. (2016). Radiation belt electron acceleration during the 17 March 2015 geomagnetic storm: Observations and simulations. *Journal of Geophysical Research: Space Physics*, *121*(6), 5520–5536. https://doi.org/10.1002/2016JA022400

Li, W., Shprits, Y. Y., & Thorne, R. M. (2007). Dynamic evolution of energetic outer zone electrons due to wave-particle interactions during storms. *Journal of Geophysical Research*, *112*(A10), A10220. https://doi.org/10.1029/2007JA012368

Lyons, L. R., & Thorne, R. M. (1973). Equilibrium structure of radiation belt electrons. *Journal of Geophysical Research*, *78*(13), 2142–2149. https://doi.org/10.1029/ja078i013p02142

Mauk, B. H., Fox, N. J., Kanekal, S. G., Kessel, R. L., Sibeck, D. G., & Ukhorskiy, A. (2012). Science objectives and rationale for the radiation belt storm Probes mission. In N. Fox & J. L. Burch (Eds.), *The Van Allen Probes mission* (pp. 3–27). Springer. https://doi.org/10.1007/978-1-4899-7433-4_2

McIlwain, C. E. (1961). Coordinates for mapping the distribution of magnetically trapped particles. *Journal of Geophysical Research*, *66*(11), 3681–3691. https://doi.org/10.1029/JZ066i011p03681

Michaelis, I., & Shprits, Y. (2023a). *ELFIN-L Level 1 ENG (Electron Losses and Fields INvestigation on board the Lomonosov satellite, Engineering data). V. 01*. GFZ Data Services. https://doi.org/10.5880/GFZ.2.7.2023.002

Michaelis, I., & Shprits, Y. (2023b). *ELFIN-L Level 1 EPD (Electron Losses and Fields INvestigation on board the Lomonosov satellite, Electron Particle Detector). V. 01*. GFZ Data Services. https://doi.org/10.5880/GFZ.2.7.2023.003

Michaelis, I., & Shprits, Y. (2023c). *ELFIN-L Level 1 PRM (Electron Losses and Fields INvestigation on board the Lomonosov satellite, Pierce-Rowe Magnetometer data). V. 01*. GFZ Data Services. https://doi.org/10.5880/GFZ.2.7.2023.004

Michaelis, I., & Shprits, Y. (2023d). *ELFIN-L Level 2 Adiabatic Invariants (Electron Losses and Fields INvestigation on board the Lomonosov satellite). V. 01*. GFZ Data Services. https://doi.org/10.5880/GFZ.2.7.2023.005

Michaelis, I., & Shprits, Y. (2023e). *ELFIN-L Level 2 EPD (Electron Losses and Fields INvestigation on board the Lomonosov satellite, Electron Particle Detector). V. 01*. GFZ Data Services. https://doi.org/10.5880/GFZ.2.7.2023.006

Millan, R. M., & Thorne, R. M. (2007). Review of radiation belt relativistic electron losses. *Journal of Atmospheric and Solar-Terrestrial Physics*, *69*(3), 362–377. https://doi.org/10.1016/j.jastp.2006.06.019

Miyoshi, Y., Hosokawa, K., Kurita, S., Oyama, S. I., Ogawa, Y., Saito, S., et al. (2021). Penetration of MeV electrons into the mesosphere accompanying pulsating aurorae. *Scientific Reports*, *11*(1), 13724. https://doi.org/10.1038/s41598-021-92611-3

Miyoshi, Y., Saito, S., Kurita, S., Asamura, K., Hosokawa, K., Sakanoi, T., et al. (2020). Relativistic electron microbursts as high-energy tail of pulsating aurora electrons. *Geophysical Research Letters*, *47*(21), e2020GL090360. https://doi.org/10.1029/2022JA030338

Orlova, K. G., & Shprits, Y. Y. (2011). On the bounce-averaging of scattering rates and the calculation of bounce period. *Physics of Plasmas*, *18*(9), 092904. https://doi.org/10.1063/1.3638137

Qin, M., Hudson, M., Li, Z., Millan, R., Shen, X., Shprits, Y., et al. (2019). Investigating loss of relativistic electrons associated with EMIC waves at low L values on 22 June 2015. *Journal of Geophysical Research: Space Physics*, *124*(6), 4022–4036. https://doi.org/10.1029/2018JA025726

Reeves, G. D., Chen, Y., Cunningham, G. S., Friedel, R. W. H., Henderson, M. G., Jordanova, V. K., et al. (2012). Dynamic radiation environment assimilation model: Dream. *Space Weather*, *10*(3), S03006. https://doi.org/10.1029/2011SW000729

Richmond, A. (1995). Ionospheric electrodynamics using magnetic apex coordinates. *Journal of Geomagnetism and Geoelectricity*, *47*(2), 191–212. https://doi.org/10.5636/jgg.47.191

Ripoll, J.-F., Loridan, V., Denton, M. H., Cunningham, G., Reeves, G., Santolík, O., et al. (2019). Observations and Fokker-Planck simulations of the L -shell, energy, and pitch angle structure of Earth's electron radiation belts during quiet times. *Journal of Geophysical Research: Space Physics*, *124*(2), 1125–1142. https://doi.org/10.1029/2018ja026111

Roederer, J. G., & Zhang, H. (2014). *Dynamics of magnetically trapped particles: Foundations of the physics of radiation belts and space plasmas*. Astrophysics and Space Science Library, Springer.

Shprits, Y., Allison, H. J., Wang, D., Drozdov, A., Szabo-Roberts, M., Zhelavskaya, I., & Vasile, R. (2022). A new population of ultra-relativistic electrons in the outer radiation zone. *Journal of Geophysical Research: Space Physics*, *127*(5),e2021JA030214. https://doi.org/10.1029/2021JA030214

Shprits, Y., Drozdov, A. Y., Spasojevic, M., Kellerman, A. C., Usanova, M. E., Engebretson, M. J., et al. (2016). Wave-induced loss of ultra-relativistic electrons in the Van Allen radiation belts. *Nature Communications*, *7*(1), 12883. https://doi.org/10.1038/ncomms12883

Shprits, Y., Kellerman, A., Aseev, N., Drozdov, A. Y., & Michaelis, I. (2017). Multi-MeV electron loss in the heart of the radiation belts. *Geophysical Research Letters*, *44*(3), 1204–1209. https://doi.org/10.1002/2016GL072258

Shprits, Y., & Michaelis, I. (2023). *ELFIN-L Level 3 EPD (Electron Losses and Fields INvestigation on board the Lomonosov satellite, Electron Particle Detector). V. 01*. GFZ Data Services. https://doi.org/10.5880/GFZ.2.7.2023.007

Shprits, Y. Y., Angelopoulos, V., Russell, C. T., Strangeway, R. J., Runov, A., Turner, D., et al. (2018). Scientific objectives of electron losses and fields INvestigation onboard Lomonosov satellite. *Space Science Reviews*, *214*(25), 25. https://doi.org/10.1007/s11214-017-0455-4

Shprits, Y. Y., Elkington, S. R., Meredith, N. P., & Subbotin, D. A. (2008). Review of modelling of losses and sources of relativistic electrons in the outer radiation belts: I. Radial transport. *Journal of Atmospheric and Solar-Terrestrial Physics*, *70*, 14.

Shprits, Y. Y., Subbotin, D., Drozdov, A., Usanova, M. E., Kellerman, A., Orlova, K., et al. (2013). Unusual stable trapping of the ultrarelativistic electrons in the Van Allen radiation belts. *Nature Physics*, *9*(11), 699–703. https://doi.org/10.1038/nphys2760

Shprits, Y. Y., Subbotin, D., & Ni, B. (2009). Evolution of electron fluxes in the outer radiation belt computed with the VERB code. *Journal of Geophysical Research*, *114*(A11), A11209. https://doi.org/10.1029/2008JA013784

Shprits, Y. Y., Subbotin, D. A., Meredith, N. P., & Elkington, S. R. (2008). Review of modelling of loses and sources of relativistic electrons in the outer radiation belt. II: Local acceleration and loss. *Journal of Atmospheric and Solar-Terrestrial Physics*, *70*(14), 1694–1713. https://doi.org/10.1016/j.jastp.2008.06.014

Shprits, Y. Y., Thorne, R. M., Friedel, R., Reeves, G. D., Fennell, J., Baker, D. N., & Kanekal, S. G. (2006). Outward radial diffusion driven by losses at magnetopause. *Journal of Geophysical Research*, *111*(A11), A11214. https://doi.org/10.1029/2006ja011657

Shumko, M., Gallardo-Lacourt, B., Halford, A. J., Liang, J., Blum, L. W., Donovan, E., et al. (2021). A strong correlation between relativistic electron microbursts and patchy aurora. *Geophysical Research Letters*, *48*(18), e2021GL094696. https://doi.org/10.1029/2021GL094696

Staples, F. A., Kellerman, A., Murphy, K. R., Rae, I. J., Sandhu, J. K., & Forsyth, C. (2022). Resolving magnetopause shadowing using multi-mission measurements of phase space density. *Journal of Geophysical Research: Space Physics*, *127*(2), e2021JA029298. https://doi.org/10.1029/2021JA029298

Subbotin, D., Shprits, Y., & Ni, B. (2010). Three-dimensional VERB radiation belt simulations including mixed diffusion. *Journal of Geophysical Research*, *115*(A3), A03205. https://doi.org/10.1029/2009JA015070

Subbotin, D. A., & Shprits, Y. Y. (2009). Three-dimensional modeling of the radiation belts using the Versatile Electron Radiation Belt (VERB) code. *Space Weather*, *7*(10), S10001. https://doi.org/10.1029/2008SW000452

Subbotin, D. A., Shprits, Y. Y., & Ni, B. (2011). Long-term radiation belt simulation with the VERB 3-D code: Comparison with CRRES observations. *Journal of Geophysical Research*, *116*(A12), A12210. https://doi.org/10.1029/2011ja017019

Thébault, E., Finlay, C. C., Beggan, C. D., Alken, P., Aubert, J., Barrois, O., et al. (2015). International geomagnetic reference field: The 12th generation. *Earth Planets and Space*, *67*(1), 79. https://doi.org/10.1186/s40623-015-0228-9

Thorne, R. M. (2010). Radiation belt dynamics: The importance of wave-particle interactions. *Geophysical Research Letters*, *37*(22), L22107. https://doi.org/10.1029/2010gl044990

Thorne, R. M., & Kennel, C. F. (1971). Relativistic electron precipitation during magnetic storm main phase. *Journal of Geophysical Research*, *76*(19), 4446–4453. https://doi.org/10.1029/ja076i019p04446

Thorne, R. M., O'Brien, T. P., Shprits, Y. Y., Summers, D., & Horne, R. B. (2005). Timescale for MeV electron microburst loss during geomagnetic storms. *Journal of Geophysical Research*, *110*, A09202. https://doi.org/10.1029/2004JA010882

Tsai, E., Artemyev, A., Zhang, X., & Angelopoulos, V. (2022). Relativistic electron precipitation driven by nonlinear resonance with whistler-mode waves. *Journal of Geophysical Research: Space Physics*, *127*(5), e2022JA030338. https://doi.org/10.1029/2022ja030338

Tu, W., Cunningham, G. S., Chen, Y., Henderson, M. G., Camporeale, E., & Reeves, G. D. (2013). Modeling radiation belt electron dynamics during GEM challenge intervals with the DREAM3D diffusion model. *Journal of Geophysical Research: Space Physics*, *118*(10), 6197–6211. https://doi.org/10.1002/jgra.50560

Tu, W., Li, X., Chen, Y., Reeves, G. D., & Temerin, M. (2009). Storm-dependent radiation belt electron dynamics. *Journal of Geophysical Research*, *114*, A02217. https://doi.org/10.1029/2008JA013480

Turner, D. L., Shprits, Y., Hartinger, M., & Angelopoulos, V. (2012). Explaining sudden losses of outer radiation belt electrons during geomagnetic storms. *Nature Physics*, *8*(3), 208–212. https://doi.org/10.1038/nphys2185

Usanova, M. E., Drozdov, A., Orlova, K., Mann, I. R., Shprits, Y., Robertson, M. T., et al. (2014). Effect of EMIC waves on relativistic and ultrarelativistic electron populations: Ground-based and Van Allen Probes observations. *Geophysical Research Letters*, *41*(5), 1375–1381. https://doi.org/10.1002/2013GL059024

Varotsou, A., Boscher, D., Bourdarie, S., Horne, R. B., Meredith, N. P., Glauert, S. A., & Friedel, R. H. (2008). Three-dimensional test simulations of the outer radiation belt electron dynamics including electron-chorus resonant interactions. *Journal of Geophysical Research*, *113*(A12), A12212. https://doi.org/10.1029/2007JA012862

Wang, D., & Shprits, Y. Y. (2019). On how high-latitude chorus waves tip the balance between acceleration and loss of relativistic electrons. *Geophysical Research Letters*, *46*(14), 7945–7954. https://doi.org/10.1029/2019GL082681

Wang, D., Shprits, Y. Y., Zhelavskaya, I. S., Effenberger, F., Castillo, A. M., Drozdov, A. Y., et al. (2020). The effect of plasma boundaries on the dynamic evolution of relativistic radiation belt electrons. *Journal of Geophysical Research: Space Physics*, *125*(5), e2019JA027422. https://doi.org/10.1029/2019ja027422

Zhang, X. J., Artemyev, A., Angelopoulos, V., Tsai, E., Wilkins, C., Kasahara, S., et al. (2022). Superfast precipitation of energetic electrons in the radiation belts of the Earth. *Nature Communications*, *13*(1), 1611. https://doi.org/10.1038/s41467-022-29291-8

References From the Supporting Information

Rodger, C. J., Carson, B. R., Cummer, S. A., Gamble, R. J., Clilverd, M. A., Green, J. C., et al. (2010). Contrasting the efficiency of radiation belt losses caused by ducted and nonducted whistler-mode waves from ground-based transmitters. *Journal of Geophysical Research*, *115*(A12), A12208. https://doi.org/10.1029/2010JA015880

Shprits, Y. Y., & Thorne, R. M. (2004). Time dependent radial diffusion modeling of relativistic electrons with realistic loss rates. *Geophysical Research Letters*, *31*(8), L08805. https://doi.org/10.1029/2004GL019591